SECURITY INFORMATION

CONFIDENTIAL

Copy 6
RM L51K02

JAN 17 1952

NACA RM L51K02

NACA

RESEARCH MEMORANDUM

TRANSONIC FLIGHT TESTS TO DETERMINE ZERO-LIFT DRAG AND PRESSURE RECOVERY OF NACELLES LOCATED AT THE WING TIPS ON A 45° SWEPTBACK WING AND BODY COMBINATION

By Sherwood Hoffman and William B. Pepper, Jr.

Langley Aeronautical Laboratory
Langley Field, Va.

CLASSIFICATION CANCELLED

Authority NACA Res. Abs. Date 5/14/56
RN 101
By [illegible] 6/4/56 See

NATIONAL ADVISORY COMMITTEE
FOR AERONAUTICS

WASHINGTON
January 11, 1952

CONFIDENTIAL

NATIONAL ADVISORY COMMITTEE FOR AERONAUTICS

RESEARCH MEMORANDUM

TRANSONIC FLIGHT TESTS TO DETERMINE ZERO-LIFT DRAG AND PRESSURE RECOVERY OF NACELLES LOCATED AT THE WING TIPS ON A 45° SWEPTBACK WING AND BODY COMBINATION

By Sherwood Hoffman and William B. Pepper, Jr.

SUMMARY

The zero-lift drag of a sweptback wing and body combination with nacelles having NACA 1-50-250 nose inlets located at the wing tips was determined by flight tests of rocket-propelled models at transonic speeds. The inlet pressure recovery at transonic speeds was determined in flight and at supersonic speeds by preflight jet tests. The wing had a sweepback angle of 45° along the quarter-chord line, an aspect ratio of 6.0, a taper ratio of 0.6, and an NACA 65A009 airfoil section in the free-stream direction. The fineness ratio of the fuselage was 10.0. Solid and ducted nacelles were used and had fineness ratios of 9.66 and 8.73, respectively.

The drags of the configuration without nacelles, with ducted nacelles, and with solid nacelles were about the same at Mach numbers from 0.8 to 1.25. A force-break Mach number of approximately 0.96 was obtained for the three models tested. The total pressure measured after diffusion was 98 percent of the free-stream total pressure at a mass-flow ratio of about 0.7 at transonic speeds.

The wing and body of the flight model had a negligible effect on the pressure recovery of the nose-inlet diffuser over the flight-test range.

INTRODUCTION

As part of a general transonic research program of the National Advisory Committee for Aeronautics to investigate the aerodynamic properties of promising aircraft configurations, the Langley Pilotless

[redacted]

Aircraft Research Division (at its testing station at Wallops Island, Va.) has tested several rocket-propelled free-flight models to determine the variations of zero-lift drag coefficient with Mach number for a high-aspect-ratio wing and body configuration with nacelles located at various positions on the wing. The preliminary tests were conducted without air flow in the nacelles to simplify the investigation. Drag data for solid nacelles located in various chordwise, vertical, and spanwise positions on a 45° sweptback wing of aspect ratio 6.0 were published in references 1 to 4.

The present investigation gives a comparison between the drags of solid and ducted nacelles located at the wing tips of the wing-body-fin combination used in the investigations reported in the foregoing references. The wing-tip location was selected from reference 2 for this investigation because of the low drag obtained for solid nacelles at the wing tips.

The inlet of the nacelle consisted of an NACA 1-50-250 nose inlet with a critical Mach number above 0.9 and a conical subsonic diffuser that had a total angle of 7°. The nacelle was proportioned to house an axial-flow turbojet engine with an afterburner.

Because of the limited number of telemeter channels that could fit into the flight model, measurements of inlet total-pressure recovery and static pressure were obtained during flight from a single total-pressure tube located near the end of the diffuser and from a single static-pressure orifice at the duct wall. Preflight jet ground tests of a more completely instrumented nacelle (with a total-pressure rake) were used to calibrate the internal flow at Mach numbers of 1.22, 1.42, 1.75, and approximately 0.8.

The Reynolds number, based on wing mean aerodynamic chord, varied from 3.8×10^6 to 7.8×10^6 for the flight tests.

SYMBOLS

A — area in duct, square feet

a — tangential acceleration, feet per second per second

C_D — drag coefficient, based on total wing plan-form area

c — wing chord, feet

g — acceleration due to gravity, 32.2 feet per second per second

H total pressure, pounds per square foot

$\bar{H}$ average total pressure, pounds per square foot

M Mach number

m mass flow through duct, slugs per second

m_o mass flow through a stream tube of area equal to inlet area under free-stream conditions, slugs per second

p static pressure, pounds per square foot

q dynamic pressure, pounds per square foot

R_e Reynolds number, based on wing mean aerodynamic chord

R gas constant

r radius of duct at measuring station, inches

S total wing plan-form area, square feet

t static temperature, degrees Rankine

W weight of model during deceleration, pounds

θ angle between flight path and horizontal

γ ratio of specific heats

x station

y ordinate, or location of total-pressure tube measured from center line of duct

Subscripts:

o free stream

d measuring station in duct

i inlet

MODELS

Details and dimensions of the flight models and the nacelles used in this investigation are given in figures 1 and 2 and tables I to IV. Photographs showing the general arrangements of the models are presented in figure 3.

Basic research configuration.- The wing-body-fin combination was similar to those investigated in references 1 to 4. The wing had a sweepback angle of 45° along the quarter-chord line, an aspect ratio of 6.0 (based on total wing plan-form area), a taper ratio of 0.6, and an NACA 65A009 airfoil section in the free-stream direction. The leading edge of the wing intersected the fuselage contour at the maximum-diameter station. The fuselage fineness ratio was 10. The ratio of total wing plan-form area to fuselage frontal area was 16.0.

Nacelles.- A comparison between the ducted nacelle and solid nacelle is given in figure 2. Each nacelle was a body of revolution having an NACA 1-50-250 nose inlet (based on data in reference 5), a cylindrical midsection, and an afterbody of NACA 111 proportions (reference 6). The fineness ratios of the ducted nacelle and the solid nacelle (including nose plug) were 8.73 and 9.66, respectively.

The inlet of the nacelle duct, as is shown in figure 2, consisted of a conical diffuser with a 0.03-inch lip radius, a total angle of 7°, and an area ratio of 1.42:1. The duct was cylindrical from the end of the diffuser to about the middle of the nacelle afterbody. At the end of the cylindrical part, the duct was contracted to form an exit area approximately 82 percent of the inlet area.

For the flight model, the center lines of the nacelles were located in the wing plane parallel to the free-stream direction at 96 percent of the semispan in order to make the outer part of the nacelle flush with the wing tip. The nose inlet was located at 82 percent of the local chord in front of the wing leading edge. A single total-pressure tube located at the center line of the duct and one static-pressure orifice were installed about 0.5 inch after the nacelle diffuser (fig. 2(d)). The pressure tubes had an inside diameter of 0.06 inch and an outside diameter of 0.09 inch.

An isolated nacelle with a total-pressure rake in the duct was used for the ground tests. Four total-pressure tubes and one static-pressure orifice were located about 0.5 inch behind the diffuser (fig. 2(c)). The total-pressure tubes were at 0, 0.42, 0.67, and 0.88 radius from the center line of the duct and supported by a symmetrical circular-arc strut 0.08 inch thick and 0.4 inch wide. The tubes had an inside diameter of 0.02 inch and an outside diameter of 0.04 inch.

TESTS AND MEASUREMENTS

The flight tests and preflight jet ground tests were performed at the Langley Pilotless Aircraft Research Station, Wallops Island, Va. Since the models without nacelles and with solid nacelles at the wing tips (models A and C, reference 2) were tested previously, it was only required to test a model with ducted nacelles at the wing tips for a comparison of the drags at zero lift.

The Reynolds number varied from approximately 3.8×10^6 at $M_o = 0.8$ to 7.8×10^6 at $M_o = 1.25$ for the flight tests and from about 4.1×10^6 at $M \sim 0.8$ to 10.2×10^6 at $M_o = 1.75$ for the preflight jet tests as is shown in figure 4.

Flight test.- Each flight model was propelled by a two-stage rocket system and launched from a rail launcher (fig. 3(a)). The first stage consisted of a 5-inch, lightweight, high-velocity aircraft rocket motor that served to accelerate the model from zero velocity to high subsonic speeds. For the second stage, a 3.25-inch Mk 7 aircraft rocket motor installed in the fuselage accelerated the model to supersonic speeds. The models were tracked by a CW Doppler velocimeter and an NACA modified SCR 584 tracking unit to determine the deceleration and flight path during coasting flight. A survey of atmospheric conditions was made by radiosonde measurements from an ascending balloon that was released at the time of launching. A two-channel telemeter installed in the nose of the fuselage transmitted a continuous record of total-pressure and static-pressure measurements from the ducted nacelle to a ground receiving station.

The values of total-drag coefficient, based on total-wing plan-form area, were calculated for decelerating flight (reference 1) with the relation

$$C_D = -\frac{W}{q_o g S}(a + g \sin \theta)$$

The pressure recovery and mass flow in the duct were obtained for flight conditions by assuming a flat total-pressure distribution in the duct based on measurements from the total-pressure tube. The expression used for the mass-flow ratio was

$$\frac{m}{m_o} = \frac{p_d M_d A_d}{p_o M_o A_i} \left[\frac{1 + \frac{\gamma - 1}{2} M_d^2}{1 + \frac{\gamma - 1}{2} M_o^2}\right]^{1/2}$$

Preflight jet tests.- The preflight jet is of the blowdown, open-jet type and can be fitted with various nozzles for testing at supersonic and subsonic Mach numbers. A description of the preflight jet and the testing technique is given in reference 7.

The ground tests were made using the 8-inch Mach number 1.22, 1.42, and 1.75 nozzles. Although the nacelle was large relative to the nozzle, shadowgraph pictures (fig. 5) show no disturbances from the nozzle entering the inlet. Since a subsonic nozzle was not available for these tests, the 8-inch, Mach number 1.22 nozzle was operated at subcritical pressures and under steady-state conditions in order to determine the flow characteristics in the nacelle at approximately a Mach number of 0.8.

The average total pressure and mass flows were determined by integration of the measured profiles (reference 8) with the following expressions

$$\bar{H} = \int_0^1 H_d \, d\left(\frac{y}{r}\right)^2$$

$$m = \left[\frac{\gamma}{gRt_o\left(1 + \frac{\gamma - 1}{2} M_o^2\right)}\right]^{1/2} A_d p_d \int_0^1 M_d \sqrt{1 + \frac{\gamma - 1}{2} M_d^2} \, d\left(\frac{y}{r}\right)^2$$

where the static pressure and the stream stagnation temperature are constant.

The mass flow through an area equivalent to the inlet area under free-stream conditions was determined from the following relation

$$m_o = \left(\frac{\gamma}{gRt_o}\right)^{1/2} p_o M_o A_i$$

Accuracy.- The accuracy of drag coefficient and Mach number for the flight tests was established from tests of three identical models in reference 1. The error in pressure measurements for the flight tests and preflight tests was based on the accuracy of the instrumentation used. The magnitude of the errors for the data presented are believed to be within the following limits:

C_D	$(0.8 \leq M < 0.95$ and $1.05 < M \leq 1.25)$	±0.0004
C_D	$(0.95 \leq M \leq 1.05)$	±0.001
M_o		±0.005
M_d		±0.01
H_d/H_o		±0.015
$\overline{H}_d/H_o$		±0.01
p/H_o		±0.015
m/m_o		±0.05

RESULTS AND DISCUSSION

Drag.- The variations of total-drag coefficient with Mach number for the configuration without nacelles, with ducted nacelles, and with solid nacelles are given in figure 6. The solid curve in figure 6 is an average C_D curve for three models without nacelles (reference 1). The data for the model with solid nacelles are taken from reference 2. The test points for the configuration with ducted nacelles represent total C_D at the values of mass flow shown in figure 7. The maximum measured value of the internal C_D (based on total wing area) of the ducted nacelles was only 0.0002, which value is less than the experimental accuracy of the flight tests.

The previous investigations (references 1 to 4) were made for solid nacelles on the premise that the nacelle-plus-interference drag would be about the same for solid and ducted nacelles. The data of reference 8 indicate that at $M = 1.25$ and $\frac{m}{m_o} = 0.7$ the external drag coefficient (based on total wing area) of the two ducted nacelles should be only 0.0006 greater than that of the solid nacelles. It is evident from figure 6 that the variation of C_D with M for this configuration with either the solid or ducted nacelles at the wing tips was about the same and also approximately equal to that of the configuration without nacelles. Unpublished data, however, indicate that most of the favorable interference causing this low nacelle drag is lost when the aspect ratio of the wing is reduced from 6.0 to 4.0.

The force-break Mach numbers of all the models tested were about 0.96.

Pressure recovery.- Figure 8(a) shows that a nearly flat total-pressure distribution was obtained behind the subsonic diffuser from ground tests at Mach numbers of 1.22, 1.42, 1.75, and approximately 0.8. Because of the flat profile, the average total pressure $\bar{H}$ was (within the accuracy of the tests) about the same as that recorded by the total-pressure tube at the center of the duct.

The variation of pressure recovery with Mach number for the flight tests and preflight jet tests is given in figure 8(b). Although the pressure recovery during flight was determined from a single pressure tube in the center of the duct (fig. 2(d)), good agreement was obtained between the pressure recoveries of the two tests at corresponding Mach numbers. This agreement indicates that the wing and body of the flight model had a negligible effect on the pressure recovery of the nose inlet at transonic speeds. The total pressure measured after diffusion was 98 percent of the free-stream total pressure at a mass-flow ratio of about 0.7 at Mach numbers from 0.8 to 1.25.

Figure 8(b) also shows a comparison of the pressure recoveries obtained for the nacelle inlet and for a similar nose inlet diffuser tested on a body in reference 8. The difference in pressure recovery between the nacelle inlet and the reference inlet, which is less efficient at supersonic speeds, can probably be accounted for by the greater diffusing angle (8.2° instead of 7°) and the greater amount of diffusion (2:1 instead of 1.42:1) in the diffuser of reference 8.

Figure 8(c) shows the variation of static pressure at the subsonic diffuser measuring station from $M_o = 0.8$ to 1.75 as determined by the two tests.

CONCLUSIONS

The results of transonic flight tests at zero lift of a wing-body configuration with nacelles having NACA 1-50-250 nose inlets located at the wing tips of a 45° sweptback wing of aspect ratio 6.0 and preflight jet tests of the nacelle at supersonic speeds are as follows:

1. The drags of the basic configuration without nacelles, with ducted nacelles, and with solid nacelles were about the same from $M_o = 0.8$ to 1.25. A force break Mach number of approximately 0.96 was obtained for the three models tested.

2. The total pressure measured after diffusion was 98 percent of the free-stream total pressure at a mass-flow ratio of about 0.7 at Mach numbers from 0.8 to 1.25

3. The wing and body of the flight model had a negligible effect on the pressure recovery of the nose-inlet diffuser over the flight-test range.

Langley Aeronautical Laboratory
National Advisory Committee for Aeronautics
Langley Field, Va.

REFERENCES

1. Pepper, William B., Jr., and Hoffman, Sherwood: Transonic Flight Tests to Compare the Zero-Lift Drag of Underslung and Symmetrical Nacelles Varied Chordwise at 40 Percent Semispan of a 45° Sweptback, Tapered Wing. NACA RM L50G17a, 1950.

2. Pepper, William B., Jr., and Hoffman, Sherwood: Comparison of Zero-Lift Drags Determined by Flight Tests at Transonic Speeds of Symmetrically Mounted Nacelles in Various Chordwise Positions at the Wing Tip of a 45° Sweptback Wing and Body Combination. NACA RM L51F13, 1951.

3. Hoffman, Sherwood: Comparison of Zero-Lift Drag Determined by Flight Tests at Transonic Speeds of Pylon, Underslung, and Symmetrically Mounted Nacelles at 40 Percent Semispan of a 45° Sweptback Wing and Body Combination. NACA RM L51D26, 1951.

4. Pepper, William B., Jr., and Hoffman, Sherwood: Comparison of Zero-Lift Drags Determined by Flight Tests at Transonic Speeds of Symmetrically Mounted Nacelles in Various Spanwise Positions on a 45° Sweptback Wing and Body Combination. NACA RM L51D06, 1951.

5. Baals, Donald D., Smith, Norman F., and Wright, John B.: The Development and Application of High-Critical-Speed Nose Inlets. NACA Rep. 920, 1948. (Formerly NACA ACR L5F30a.)

6. Abbott, Ira H.: Fuselage-Drag Tests in the Variable-Density Wind Tunnel: Streamline Bodies of Revolution, Fineness Ratio of 5. NACA TN 614, 1937.

7. Faget, Maxime A., Watson, Raymond S., and Bartlett, Walter A., Jr.: Free-Jet Tests of a 6.5-Inch-Diameter Ram-Jet Engine at Mach Numbers of 1.81 and 2.00. NACA RM L50L06, 1951.

8. Sears, Richard I., and Merlet, C. F.: Flight Determination of the Drag and Pressure Recovery of an NACA 1-40-250 Nose Inlet at Mach Numbers from 0.9 to 1.8. NACA RM L50L18, 1951.

TABLE I

FUSELAGE COORDINATES

x (in.)	y (in.)
0	0
.4	.185
.6	.238
1.0	.342
2.0	.578
4.0	.964
6.0	1.290
8.0	1.577
12.0	2.074
16.0	2.472
20.0	2.772
24.0	2.993
28.0	3.146
32.0	3.250
36.0	3.314
40.0	3.334
44.0	3.304
48.0	3.219
52.0	3.037
56.0	2.849
60.0	2.661
64.0	2.474
66.7	2.347

TABLE II

COORDINATES OF THE NACA 65A009 AIRFOIL

x/c (percent)	y/c (percent)
0	0
.5	.688
.75	.835
1.25	1.065
2.5	1.460
5.0	1.964
7.5	2.385
10.0	2.736
15.0	3.292
20.0	3.714
25.0	4.036
30.0	4.268
35.0	4.421
40.0	4.495
45.0	4.485
50.0	4.377
55.0	4.169
60.0	3.874
65.0	3.509
70.0	3.089
75.0	2.620
80.0	2.117
85.0	1.594
90.0	1.069
95.0	.544
100.0	.019
Leading-edge radius, 0.58 percent c	

TABLE III

COORDINATES FOR SOLID NACELLE

x (in.)	y (in.)
0	0
.100	.070
.330	.169
.830	.336
1.330	.489
1.830	.622
2.330	.747
2.580	.800
2.958	.876
3.585	.974
4.840	1.105
6.095	1.190
7.350	1.240
8.605	1.255
16.830	1.255
17.872	1.237
18.913	1.195
19.955	1.127
20.996	1.029
22.038	.909
23.079	.768
24.121	.616
24.250	.598

TABLE IV

COORDINATES FOR DUCTED NACELLE

x (in.)	y (in.)
0	0.661
.063	.723
.188	.770
.251	.789
.439	.836
.628	.876
1.255	.974
2.196	1.077
3.138	1.152
4.393	1.219
6.275	1.255
14.500	1.255
15.542	1.237
16.583	1.195
17.625	1.127
18.666	1.029
19.708	.909
20.749	.768
21.791	.616
21.920	.598
Lip radius = 0.03 inch	

[redacted]

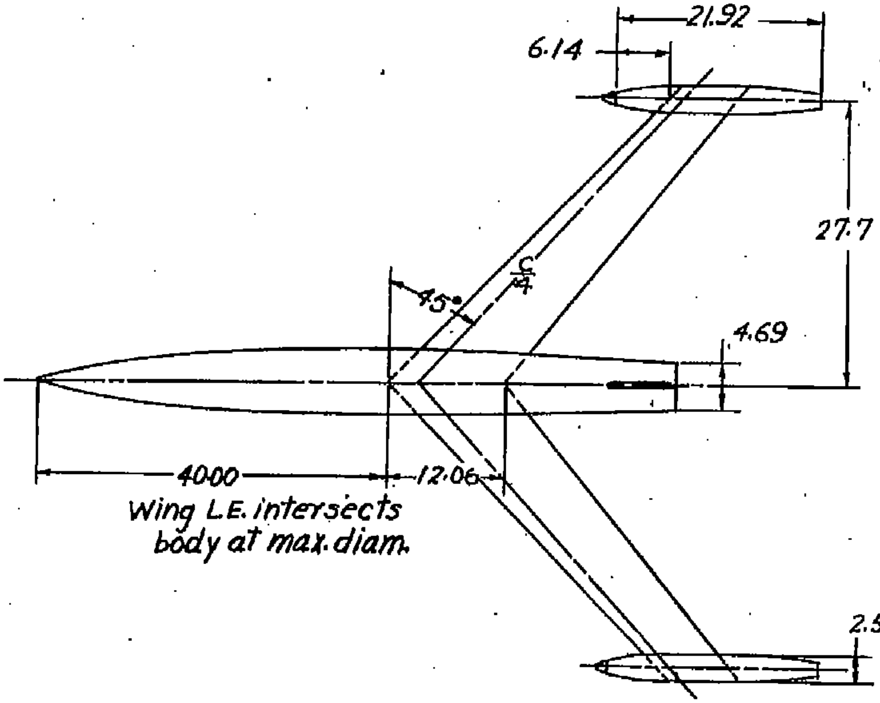

Model characteristics:

Body fineness ratio	10.0
Wing aspect ratio	6.0
Wing taper ratio	0.6
Mean aerodynamic chord, ft	0.822
Airfoil parallel to free stream	NACA 65A009
Total wing plan-form area, sq ft	3.878
Exposed wing plan-form area, sq ft	3.333
Exposed wing frontal area, sq ft	0.299
Body frontal area, sq ft	0.242
Total frontal area, sq ft	0.550
Exposed fin plan-form area (2 fins), sq ft	0.468

Fins are flat plates and 0.091 inch thick with 0.045-inch radius at edges.

Nacelle fineness ratio (ducted)	8.73
Nacelle fineness ratio (solid)	9.66
Frontal area of one nacelle, sq ft	0.094
Nose inlet of nacelle	NACA 1-60-250

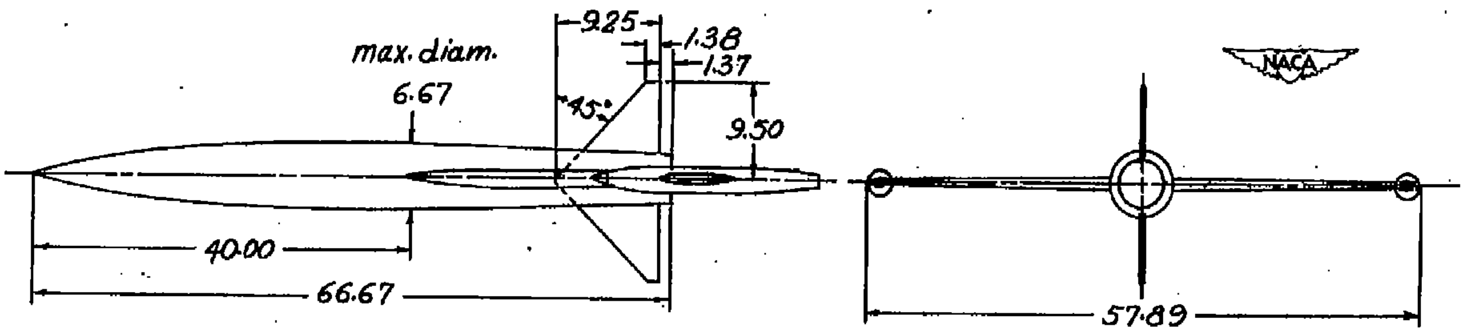

Figure 1.- General arrangement and dimensions of test model. All dimensions are in inches.

SECURITY INFORMATION

[redacted]

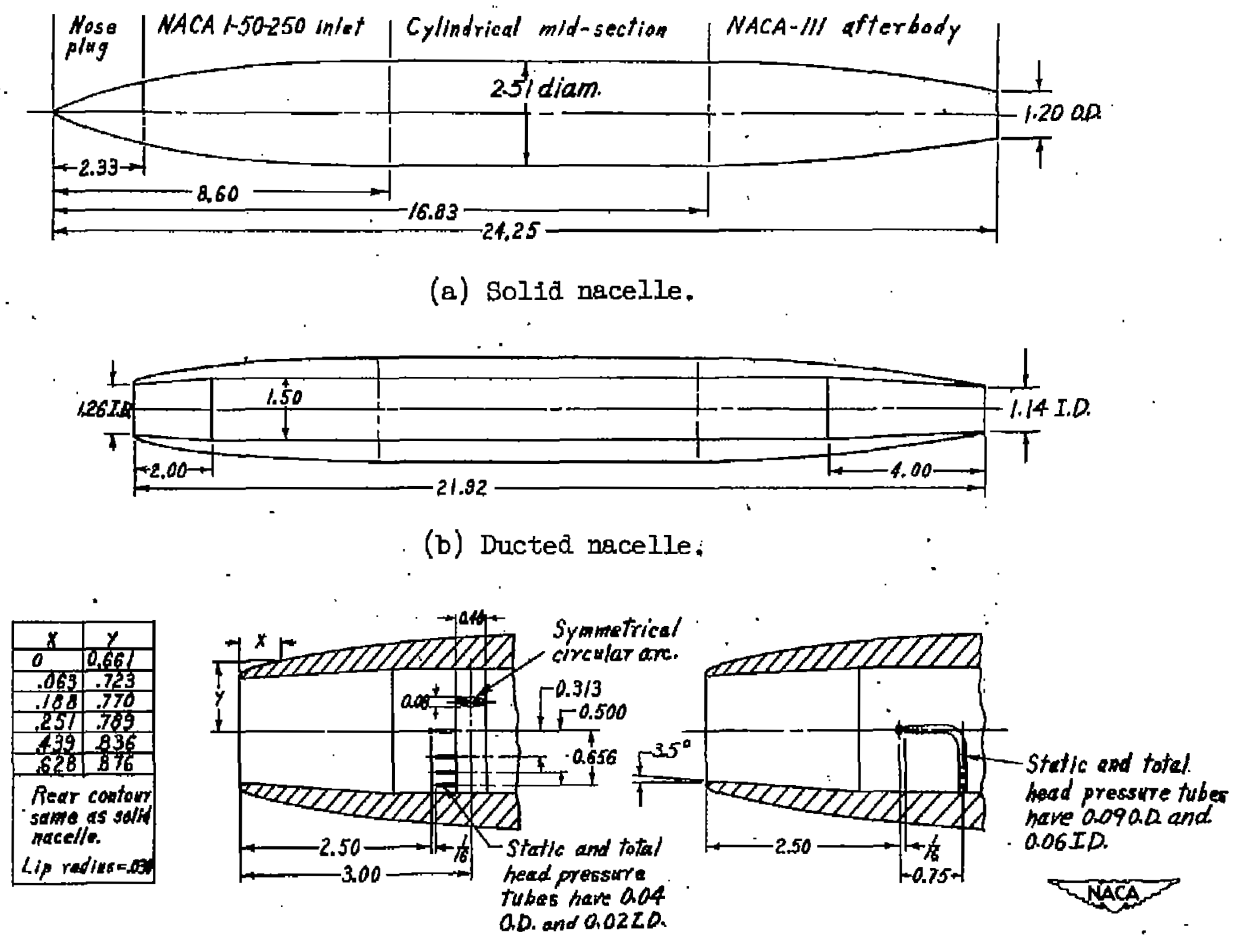

(c) Inlet for ground test. (d) Inlet for flight test.

Figure 2.- Details and dimensions of solid nacelle, ducted nacelle, and nacelle inlets used for the ground tests and flight tests. All dimensions are in inches.

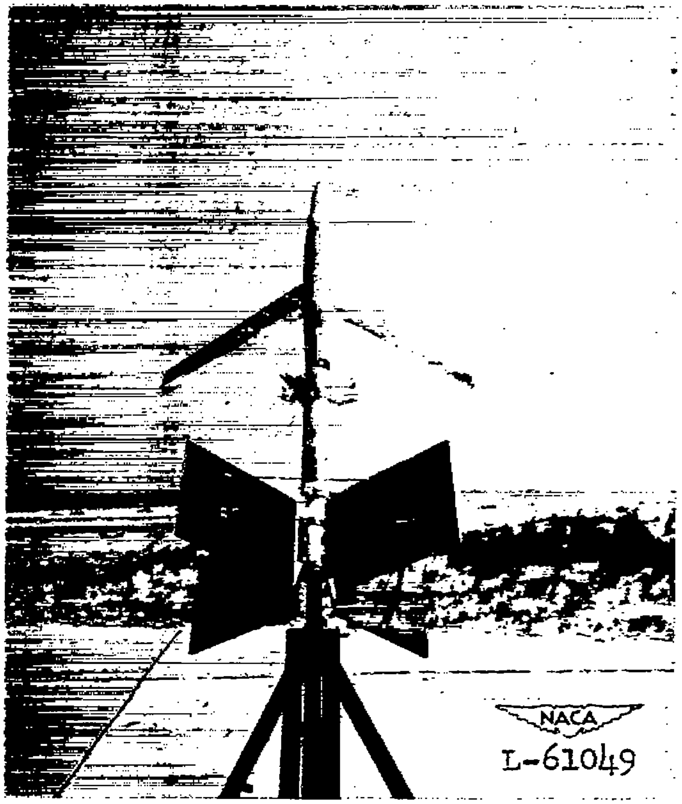

(a) Test model without nacelles. Model and booster arrangement on rail launcher.

Figure 3.- General views of test models.

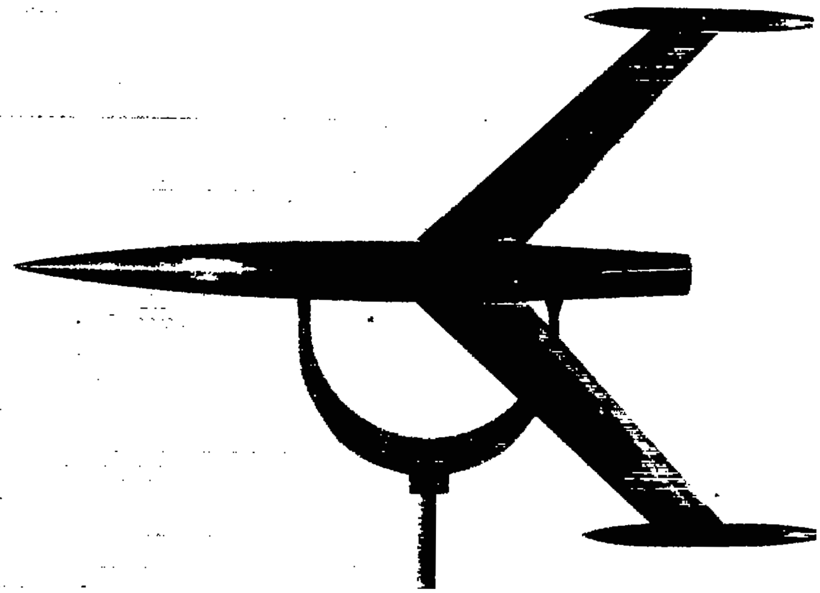

(b) Flight model with solid nacelles.

NACA
L-67573

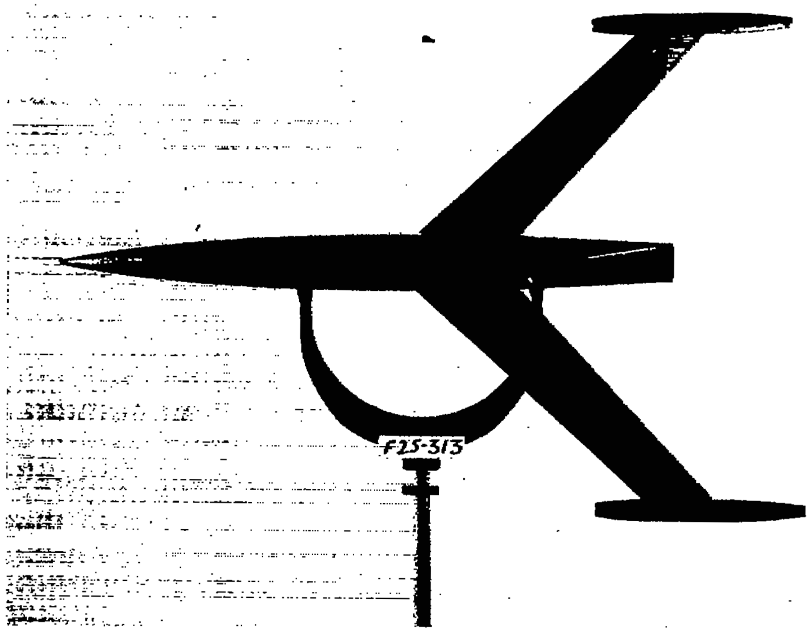

(c) Flight model with ducted nacelles.

NACA
L-69938

Figure 3.- Concluded.

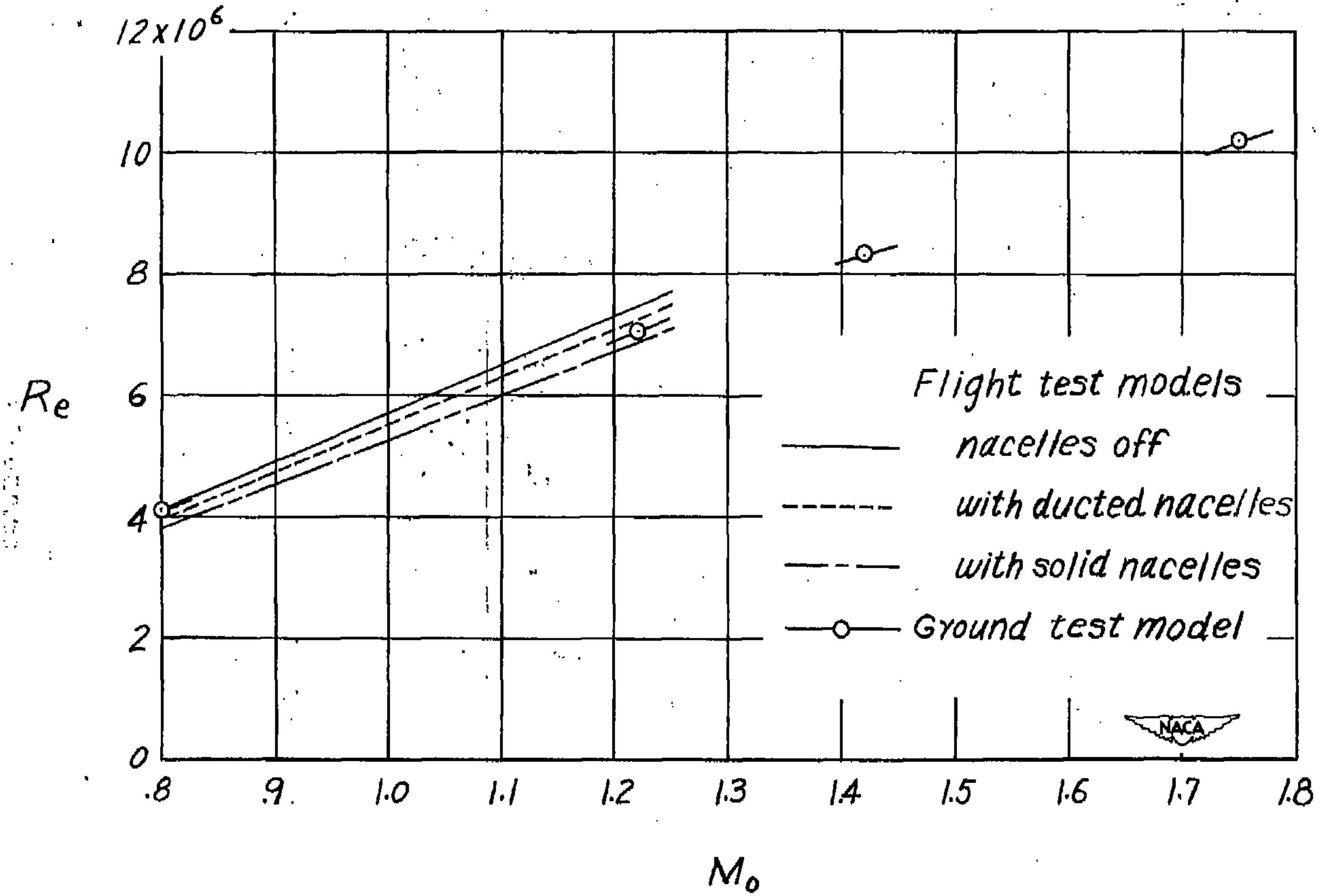

Figure 4.- Variation of Reynolds number with Mach number for models tested. Reynolds number based on wing mean aerodynamic chord.

SECURITY INFORMATION

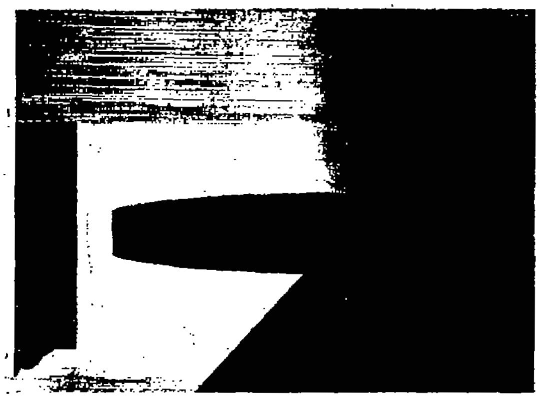

(a) M = 1.22.

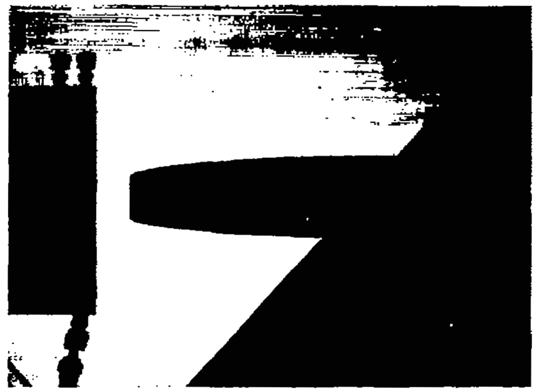

(b) M = 1.42.

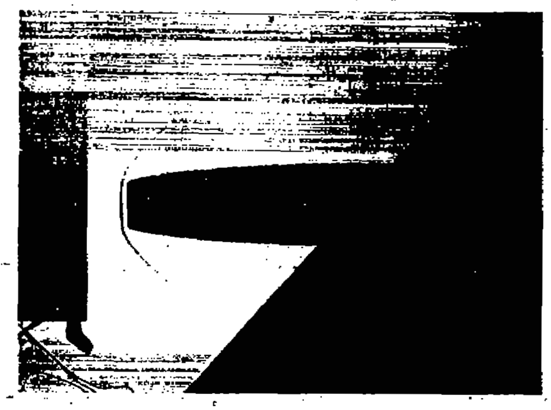

L-70845

(c) M = 1.75.

Figure 5.- Shadowgraphs of NACA 1-50-250 nose inlet in preflight jet.

[redacted]

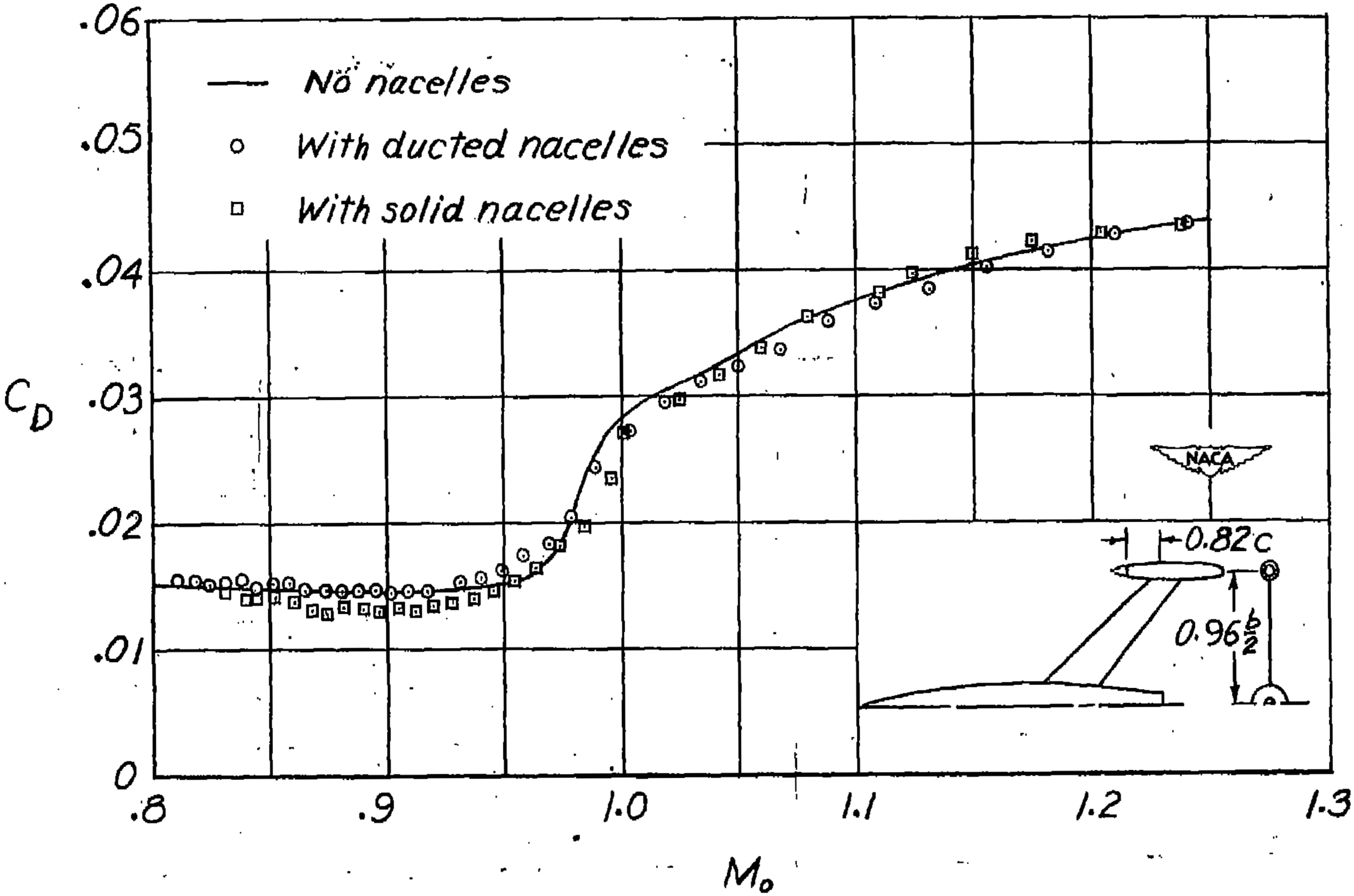

Figure 6.- Variation of drag coefficient with Mach number for models without nacelles, with ducted nacelles, and with solid nacelles.

[redacted]

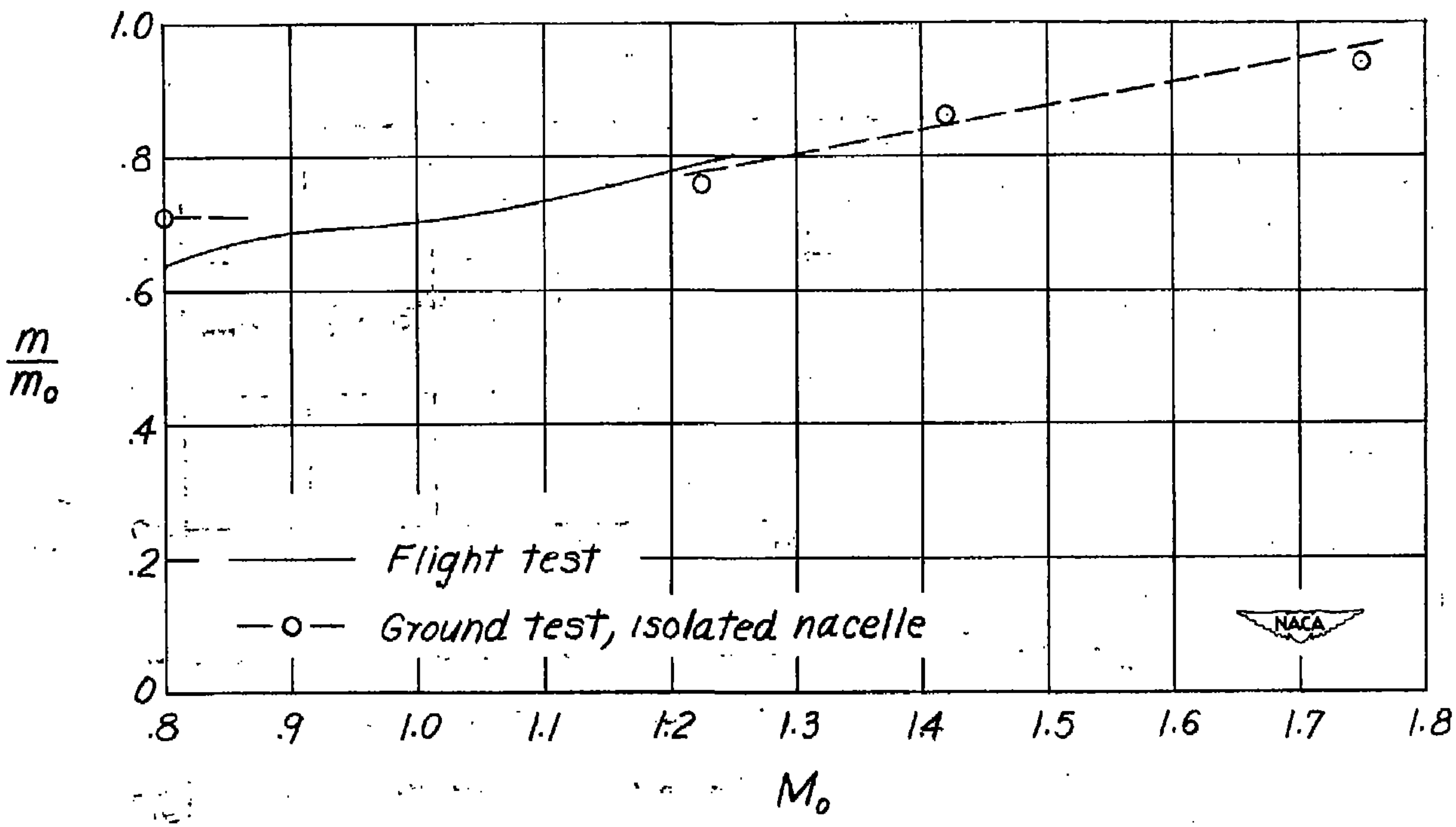

Figure 7.- Variation of mass-flow ratio with Mach number.

[redacted]

[redacted]

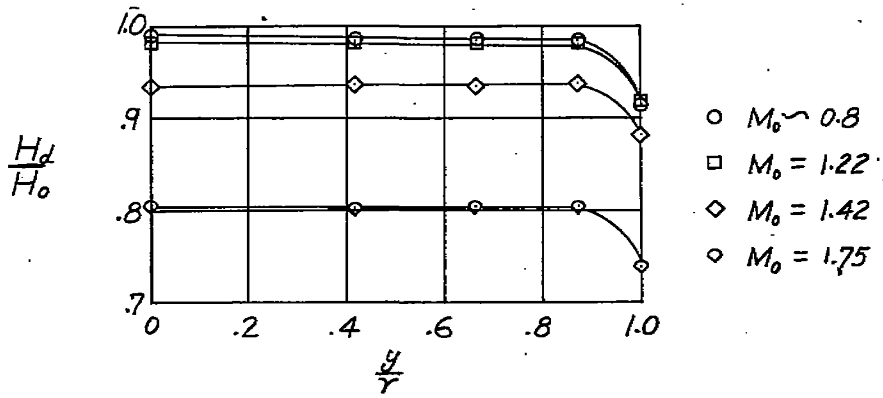

(a) Total-pressure profile at diffuser for several Mach numbers as determined by ground tests of the isolated nacelle.

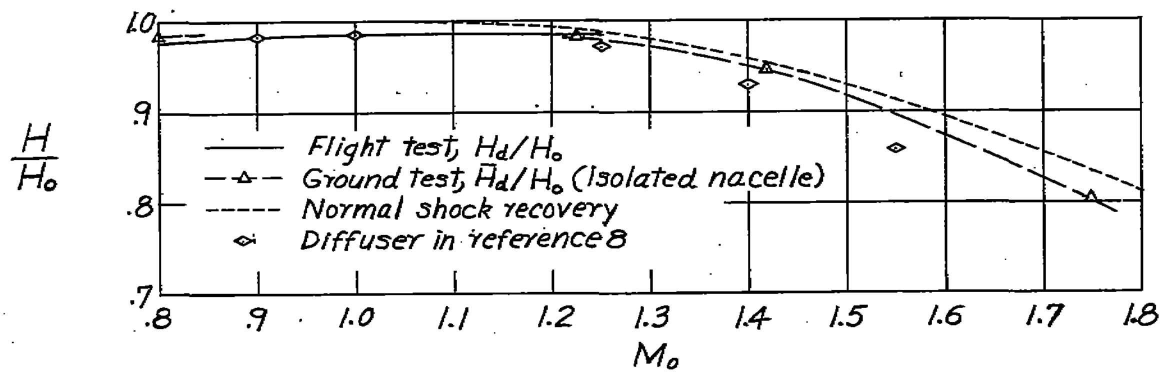

(b) Variation of diffuser pressure recovery with Mach number.

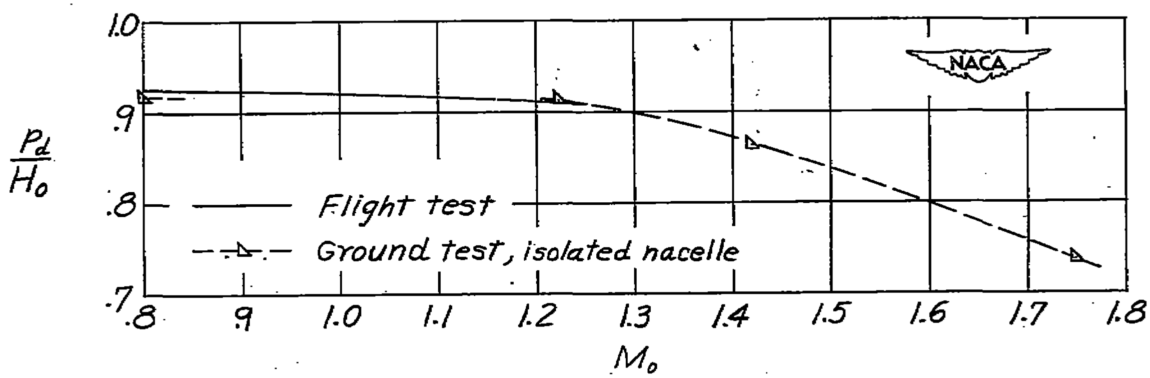

(c) Variation of static pressure in diffuser with Mach number.

Figure 8.- Properties of ducted nacelle with an NACA 1-50-250 inlet as determined by flight tests and ground tests.

[redacted]

SECURITY INFORMATION

[redacted]